

Investigating the Cell Division Protein FtsZ and its Regulation in *Bacillus subtilis*

Phoebe Coral Peters

A thesis submitted in fulfillment of the
requirements for the degree of
Doctor of Philosophy



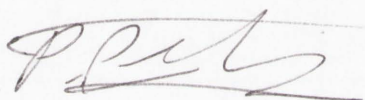
Institute for the Biotechnology of Infectious Diseases
University of Technology, Sydney
NSW, Australia

December 2008

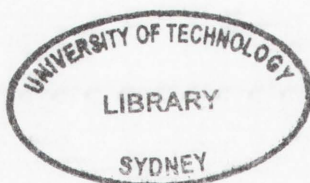
Certificate of Authorship/Originality

I certify that the work in this thesis has not previously been submitted for a degree nor has it been submitted as part of requirements for a degree except as fully acknowledged within the text.

I also certify that the written preparation of the thesis, and all experimental work associated with it, has been carried out solely by me, unless otherwise indicated. Finally, I certify that all information sources and literature used are acknowledged in the text.



Phoebe Coral Peters
December 2008



Acknowledgements

These past few years have certainly been thoroughly enjoyable and stimulating and for that there are many people to acknowledge. Firstly I wish to thank a thousand times over my supervisor, Associate Professor Liz Harry. She provided me with a fabulous and fascinating project, and her guidance, support and advice were invaluable throughout, one could simply not ask for more in a supervisor. Liz always encouraged me to take opportunities and infused into me the confidence to truly develop as a scientist. I also owe her further thanks for reading and re-reading this thesis, teaching me to craft my arguments and refine my expression of the written word.

The people of the Harry lab have always provided friendship and invaluable assistance and I sincerely thank them all for creating such a wonderful and inspiring environment; Gerry Wake, Rowena Lock, Rebecca Rashid, Lyndal Thompson, Torsten Theis, Kate Michie, Marcelle Freeman, Margaret Migocki, Kylie Turner, Patricia Quach, Leigh Monahan, Adeline Koay, Ana Porta-Cubas, Jo Packer, Christopher Rodrigues, Jo Santos, and all the honours students. The wealth of knowledge and experience concentrated into one lab was awe-inspiring, and there was always someone happy to help. Just as importantly there was constantly a friendly face ready with a smile, word of encouragement, or an excuse to get a cup of tea and do the crossword. Particularly I thank Pat (the queen of formatting), Leigh (the king of editing) and Packer for being such tremendous people to both play and work with.

I am greatly indebted to Shigeki Moriya, who taught me so much about being a scientist, about life in general, and of course provided valued antibodies. I am grateful to Arne Müller (Carl Zeiss) for technical assistance with 3D deconvolution, time-lapse imaging and image analysis, and Fraser Torpy for performing statistical analyses. I thank Professor Guy Cox and Carola Thoni for their companionship in Germany and along with the Leica STED team, Ulf Schwarz, Jochen Sieber and Tanjef Szellas, for their know-how and technical expertise in microscopy. I also thank the FABLS network for funding these ventures to

Germany. For the priceless gift of strains I acknowledge Laurent Janniere, Petra Levin and Frederico Gueiros-Filho.

Just as importantly, on a personal note I would like to thank my **fiancé**, Cameron Jennings, without his smile to enliven each and every day, I simply would not have made it through. With my whole heart I thank him for being the simply wonderful person that he is, for proofreading this dissertation and for being an all round super-genius. Special thanks goes to my parents and family for their patience and unending patronage throughout my lengthy uni education, and to my friends, particularly Kate, Heather and Peta, who have provided much needed distractions and laughs.

Lastly, I would like to acknowledge the financial assistance provided by the University of Technology, Sydney in the form of an IBID Postgraduate Scholarship.

Table of Contents

Certificate of Authorship/Originality ii

Acknowledgements iii

Table of Contents..... v

Table of Figures x

Table of Tables xv

Publications..... xvi

Abbreviations..... xviii

Abstract..... xxii

Chapter 1. Introduction..... 1

1.1 Preface 1

1.2 The model organism: *Bacillus subtilis* 2

1.2.1 Sporulation and the spore outgrowth system 4

1.3 DNA replication..... 5

1.3.1 Initiation of DNA replication..... 7

1.3.2 DNA chain elongation 8

1.4 The cell division protein, FtsZ, and the Z ring 10

1.4.1 FtsZ 11

1.4.2 The Z ring 12

1.4.3 Biochemistry of FtsZ and the Z ring 13

1.4.4 Positioning the Z ring 16

1.5 FtsZ accessory proteins and the divisome..... 17

1.5.1 FtsA..... 20

1.5.2 ZapA..... 21

1.6 Regulation of cell division..... 22

1.6.1 The Min system 24

1.6.2 Nucleoid occlusion 27

1.6.3 The coordination between DNA replication and cell division 29

1.7 The cytoskeletal network..... 31

1.8 Bacterial pathway coupling..... 33

1.9 Thesis aims 34

Chapter 2. Material and Methods..... 37

2.1 Chemicals, reagents and solutions 37

2.2 *B. subtilis* strains and growth conditions..... 38

2.2.1	Testing the status of the <i>amyE</i> locus of <i>B. subtilis</i>	40
2.3	Preparation and transformation of competent <i>B. subtilis</i> cells.....	40
2.4	Construction of the <i>minCD</i> deletion strain	41
2.5	Preparation, germination and outgrowth of <i>B. subtilis</i> spores	41
2.6	General DNA methods.....	42
2.6.1	Purification of chromosomal DNA from <i>B. subtilis</i>	42
2.6.2	Agarose gel electrophoresis of DNA.....	42
2.6.3	Determination of DNA concentration	43
2.6.4	Polymerase chain reaction (PCR) and oligonucleotides	43
2.6.5	DNA sequencing	44
2.7	Microscopy methods	45
2.7.1	Immunofluorescence microscopy (IFM).....	45
2.7.2	3D deconvolution.....	47
2.7.3	Ethanol fixation of cells and nucleoid visualisation	47
2.7.4	Preparation for live cell fluorescence microscopy.....	48
2.7.4.1	Time-lapse of live fluorescence cells	48
2.7.5	Phase contrast and fluorescence microscopy.....	49
2.7.6	Cell scoring and statistics.....	50
2.7.7	Confocal microscopy	50
2.8	Antibody conjugation and STED Microscopy	51
2.8.1	Fourier transform analysis	52
2.9	Western blot analysis	52
2.9.1	Whole cell protein extraction for Western blotting	52
2.9.2	Bradford assay for protein concentration	52
2.9.3	Denaturing SDS-polyacrylamide gel electrophoresis (SDS-PAGE) of proteins	53
2.9.4	Western transfer.....	54
2.9.5	Immunodetection	54
2.10	Measuring DNA synthesis using tritiated thymine	54
2.11	Suppliers of chemicals, reagents and equipment	55
Chapter 3. Investigating the Coordination of Cell Division with DNA		
Replication		57
3.1	Introduction	57
3.1.1	Linking cell division and DNA replication	57
3.1.2	The drug 6-(p-hydroxyphenylazo)-uracil (HPUra)	59
3.1.3	Chapter aims	61
3.2	Results	62
3.2.1	Construction of an HPUra-resistant strain.....	62
3.2.2	Nucleoid staining and examination of DNA replicative ability.....	64
3.2.2.1	DAPI staining of SU8 and SU473 (HPUra ^R) in the presence and absence of HPUra.....	64
3.2.2.2	Measuring DNA synthesis using tritiated thymine incorporation	66
3.2.3	Z ring formation and positioning	69
3.2.3.1	Control strains SU8 and SU5.....	70
3.2.3.2	HPUra resistant strain SU473 (HPUra ^R).....	71
3.3	Discussion.....	75

3.3.1	Z rings form centrally in the presence of HPUra in a resistant strain	75
3.3.2	How is Z ring assembly coordinated with DNA replication?	78
3.3.3	What role does the nucleoid play?	80

Chapter 4. Investigations into the Formation of FtsZ Helical Structures During the Cell Cycle..... 85

4.1	Introduction	85
4.1.1	The assembly pathway for Z ring formation	85
4.1.2	Non-ring polymers of FtsZ can form under aberrant conditions	87
4.1.3	Chapter aims	90
4.2	Results	92
4.2.1	FtsZ forms a helical structure during vegetative growth	92
4.2.1.1	Three dimensional imaging of the FtsZ helical localization	93
4.2.1.2	Fluorescence intensity quantification of the FtsZ helix	96
4.2.1.3	FtsZ antibody binds specifically to the FtsZ protein	97
4.2.2	The helical assembly of FtsZ forms prior to the Z ring	98
4.2.3	The helical structure of FtsZ in live cells	101
4.2.4	The FtsZ helical structure is highly dynamic	103
4.2.4.1	Development of time-lapse microscopy technique	105
4.2.4.2	Dynamics of FtsZ within live cells	107
4.2.5	Cell cycle analysis of FtsZ localization in live cells	109
4.2.5.1	Time-lapse of SU434 in vegetatively growing cells	112
4.2.6	Helical dynamics of FtsZ confirmed using alternative fluorescence fusion proteins	117
4.2.6.1	FtsZ-GFP driven by the native promoter	117
4.2.7	The cell division protein, FtsA, also forms a pre-divisional helical structure	125
4.2.8	Do the cell division proteins FtsZ and FtsA co-localize?	126
4.2.9	The cell division protein ZapA also forms short helices at midcell	130
4.2.9.1	IFM on SU557 (GFP-ZapA) confirms the absence of an extended helix	135
4.3	Discussion	138
4.3.1	A new model for midcell Z ring formation	138
4.3.2	FtsA may act as a tether to the membrane for both Z rings and Z helices	141
4.3.3	What is involved in the dynamic regulation of FtsZ?	142
4.3.4	FtsZ assembly and its regulation by the Min system and nucleoid occlusion	143
4.3.5	The relationship between the FtsZ helix and the rod-shaped cell	144
	Supplementary DVD figure legends:	146

Chapter 5. Investigations into the Regulation of the FtsZ Helix by the Min System..... 149

5.1	Introduction	149
5.1.1	Division regulation: the Min system	150
5.1.1.1	MinC, MinD and the MinCD complex	150
5.1.1.2	The topological regulator, DivIVA	153
5.1.1.3	The Min system and Z ring precision	155
5.1.2	Chapter aims	156
5.2	Results	158
5.2.1	Construction of MinCD over-expression strain SU573	158
5.2.1.1	Strain construction	158
5.2.1.2	Confirmation of MinCD over-expression phenotype	159
5.2.2	Controlling the amount of MinCD overproduced during vegetative growth	161

5.2.2.1	Western blot detection of the MinD protein in vegetatively growing cells	162
5.2.3	FtsZ still forms a long helix when MinCD is over-expressed in outgrowing spores	164
5.2.4	The long FtsZ helix can also form in vegetative cells over-expressing MinCD	168
5.2.4.1	3D deconvolution of FtsZ helical localization in the presence of MinCD over-expression.....	170
5.2.5	Construction of MinCD deletion strains	172
5.2.6	MinCD ⁻ strains form minicells and polar Z rings.....	175
5.2.7	Immunofluorescence microscopy (IFM) of vegetative cells to examine FtsZ in the absence of the Min system.....	176
5.2.7.1	3D deconvolution of FtsZ helical localization in the absence of the Min system	178
5.2.8	FtsZ localization using outgrown spores of SU556 (MinCD ⁻ FtsZ-YFP) and SU560 (MinCD ⁻)	180
5.2.8.1	Examination of FtsZ localization by IFM in SU560 (MinCD ⁻) cells	180
5.2.8.2	Live visualisation of FtsZ-YFP localization in SU556 (MinCD ⁻ FtsZ-YFP).....	183
5.2.9	Dynamic localization revealed through time-lapse studies of FtsZ-YFP in the absence of the Min system	185
5.2.9.1	Short-interval time-lapse of FtsZ-YFP in the absence of the Min system	185
5.2.9.2	FtsZ-FYP in the absence of the Min system assembles into a polar Z ring via a short helical intermediate	186
5.2.10	Do the polar Z rings go on to constrict and facilitate cell division?	194
5.2.10.1	Extended imaging in SU556 (MinCD ⁻ FtsZ-YFP) outgrowing spores	194
5.2.10.2	Time-lapse imaging in SU556 (MinCD ⁻ FtsZ-YFP) vegetatively growing cells	196
5.2.11	Summary of time-lapse analysis of FtsZ-YFP dynamics in the absence of the Min system.....	198
5.2.12	Further assessment of FtsZ localization (using FtsZ-GFP) in live vegetatively growing cells over-expressing MinCD	201
5.2.13	Using outgrown spores of SU593 (MinCD ⁺⁺ FtsZ-GFP) to examine FtsZ localization during the first cell cycle in live cells	205
5.2.13.1	Is MinCD over-expressed at early time points in outgrown spores?	205
5.2.13.2	FtsZ localization in live SU593 spores germinated and outgrown without IPTG.....	207
5.2.13.3	Live SU593 spores germinated and outgrown with IPTG to induce MinCD over-expression.....	208
5.2.14	Dynamic localization of FtsZ-GFP in SU593 (MinCD ⁺⁺ FtsZ-GFP) outgrown spores.....	212
5.2.14.1	Control time-lapse in outgrown SU593 (MinCD ⁺⁺ FtsZ-GFP) without induction of MinCD over-expression.....	212
5.2.14.2	Time-lapse studies in outgrown SU593 (MinCD ⁺⁺ FtsZ-GFP) with 1 mM IPTG to induce over-expression of MinCD	214
5.2.14.3	Summary of time-lapse analysis of FtsZ-GFP dynamics in the presence and absence of MinCD over-expression.....	219
5.2.15	Examination of the localization of MinC/D by IFM	221
5.3	Discussion.....	223
5.3.1	Further evidence for a new model of Z ring formation	223
5.3.2	The Min system and FtsZ.....	225
5.3.3	The emerging importance of lateral associations between FtsZ protofilaments	228
5.3.4	A model for the relationship between the short FtsZ helix and the Z ring involving lateral associations	229
5.3.5	What is the purpose of the extended helix?	231
	Supplementary DVD figure legends:	233

Chapter 6. Investigating Advanced Techniques in Bacterial Microscopy . 237

6.1	Introduction.....	237
------------	--------------------------	------------

6.1.1	4Pi Microscopy increases axial resolution	238
6.1.2	STED Microscopy increases lateral resolution	239
6.1.3	Chapter aims	243
6.2	Results	245
6.2.1	4Pi Microscopy	245
6.2.1.1	4Pi slide preparation	245
6.2.1.2	Testing slides for transportation to Germany	247
6.2.1.3	4Pi imaging in Germany	247
6.2.2	Testing a new fluorescent conjugate, Alexa 488	249
6.2.3	STED Microscopy	251
6.2.3.1	Preparation of the ATTO antibody conjugate	252
6.2.3.2	Testing the fluorescence of the ATTO 647N dye	254
6.2.3.3	Determining the optimal mounting media for STED imaging	256
6.2.4	Imaging using the STED super-resolution microscope	257
6.2.4.1	Analysis of STED images using intensity graphs	259
6.2.4.2	Fourier transform analysis of STED images	262
6.2.5	Is the discontinuous FtsZ helix an artifact?	265
6.2.5.1	TDE as an effective mounting medium	267
6.2.6	Comparison of theoretical STED parameters and actual parameters	268
6.3	Discussion	270
6.3.1	4Pi microscopy reveals unexpected bleaching	270
6.3.2	STED microscopy provides further detail for the new model of Z ring and helix formation	271
6.3.3	STED microscopy reveals enhanced resolution of the FtsZ helix	274
6.3.4	Further advances in microscopical imaging	276
	Chapter 7. General Discussion	279
	References	287

Table of Figures

Figure 1.1 Electron micrograph of *B. subtilis* undergoing cell division.2

Figure 1.2 The cell cycle of *B. subtilis*.3

Figure 1.3 Simplified *B. subtilis* cell cycle, depicting one round of DNA replication.6

Figure 1.4 Simplified representation of initiation of DNA replication in *B. subtilis*.7

Figure 1.5 Simplified cartoon portraying elongation of DNA replication in *B. subtilis*.10

Figure 1.6 Z ring morphology in a wild type *B. subtilis* cell.12

Figure 1.7 FtsZ and the formation of the Z ring.14

Figure 1.8 Proteins involved in cell division and their assembly pathway in *E. coli* and *B. subtilis*.19

Figure 1.9 Ribbon plot of the crystal structure of FtsA from *Thermotoga maritima*.20

Figure 1.10 Model for the function of ZapA in Z ring formation.22

Figure 1.11 Schematic of the Min system and nucleoid occlusion (NO) in *B. subtilis*.23

Figure 1.12 The Min system in *B. subtilis* and *E. coli*.26

Figure 1.13 A schematic overview of the major events during one cycle of bacterial cell division.31

Figure 1.14 Model for shape control by MreB and Mbl.32

Figure 1.15 Outline of the multiple points of coordination that exist between cell cycle events.33

Figure 3.1 Schematic of how HPURA derives its inhibitory ability.60

Figure 3.2 DNA sequencing of the HPURA mutation site in the *polC* gene.63

Figure 3.3 DAPI staining of *B. subtilis* strains SU8 and SU473 (HPURA^R) in the absence and presence of HPURA.65

Figure 3.4 DAPI staining of *B. subtilis* strain SU5 in the absence and presence of HPURA.67

Figure 3.5 Graph of thymine incorporation into SU5 and SU473 (HPURA^R).69

Figure 3.6 IFM images of *B. subtilis* strains SU8 and SU473 (HPURA^R) in the absence and presence of HPURA.72

Figure 3.7 Z ring positioning of *B. subtilis* strains SU8, SU5 and SU473 (HPURA^R) in the absence and presence of HPURA.73

Figure 3.8 Diagram of the *B. subtilis* replication fork in the absence and presence of HPURA.76

Figure 3.9 Position of the genes on the circular *B. subtilis* chromosome.77

Figure 3.10 Demonstrative nucleoid conformations in *B. subtilis* cells where DNA replication is inhibited.83

Figure 3.11 Midcell Z ring positioning in rod-shaped bacteria.83

Figure 4.1 FtsZ assembly model.86

Figure 4.2 Helix formation in *E. coli* with the mutant temperature sensitive protein FtsZ26 at the permissive temperature.88

Figure 4.3 FtsZ helices in *E. coli*.89

Figure 4.4 FtsZ helices during entry into sporulation in *B. subtilis*.90

Figure 4.5 Immunofluorescence analysis of FtsZ localization in vegetative wild type *B. subtilis*.93

Figure 4.6 Projected two-dimensional images of FtsZ structures in cells obtained by 3D deconvolution.94

Figure 4.7 Three-dimensional maximum image projections of FtsZ structures in cells obtained by confocal microscopy..... 95

Figure 4.8 Quantitation of FtsZ-immunostaining intensity of the FtsZ helical structures in cells that contained a Z ring and in those that did not..... 97

Figure 4.9 Testing specificity of the FtsZ antibody. 98

Figure 4.10 Cell Length distribution of vegetatively growing wild type *B. subtilis* cells. .. 99

Figure 4.11 FtsZ-immunofluorescence staining of methanol fixed SU5 outgrown spores. 101

Figure 4.12 Visualisation of FtsZ-YFP in cells outgrown from spores. 103

Figure 4.13 Immunofluorescence analysis of FtsZ localization to confirm helical pattern in cells expressing FtsZ-YFP. 105

Figure 4.14 Phase contrast time-lapse microscopy of outgrown spores. 106

Figure 4.15 Time-lapse microscopy showing dynamics of FtsZ-YFP localization in outgrown spores. 108

Figure 4.16 Short interval time-lapse microscopy of FtsZ-YFP localization in outgrown spores..... 108

Figure 4.17 Time-lapse microscopy of FtsZ-YFP localization over an entire cell cycle in outgrown spores. 110

Figure 4.18 Spatial dynamics of FtsZ-YFP localization within the cell. 111

Figure 4.19 Time-lapse images of FtsZ-YFP localization in SU434 vegetatively growing cells. 1 μ m..... 114

Figure 4.20 Spatial dynamics of FtsZ-YFP localization within a vegetatively growing cell. 115

Figure 4.21 Time-lapse images of FtsZ-YFP short helical localization in SU434 vegetatively growing cells..... 116

Figure 4.22 Live fluorescence analysis of FtsZ-GFP localization..... 119

Figure 4.23 Visualisation of FtsZ-GFP in cells outgrown from spores. 120

Figure 4.24 Time-lapse images of FtsZ-GFP localization in SU570 (FtsZ-GFP) in outgrown spores at 30°C. 121

Figure 4.25 Time-lapse images of FtsZ-GFP localization in SU570 (FtsZ-GFP) in outgrown spores at 25°C..... 122

Figure 4.26 Short interval time-lapse images of FtsZ-GFP localization in SU570 (FtsZ-GFP) vegetative cells. 124

Figure 4.27 Immunofluorescence visualisation of FtsA in vegetatively growing cells. 126

Figure 4.28 FtsZ and FtsA localization by immunofluorescence.. 127

Figure 4.29 Immunofluorescence analysis of FtsZ and FtsA co-localization..... 128

Figure 4.30 Immunofluorescence analysis of FtsZ and FtsZ-YFP co-localization.. 130

Figure 4.31 Live fluorescence analysis of GFP-ZapA localization. 131

Figure 4.32 Time-lapse images of GFP-ZapA localization in SU557 in outgrown spores. 133

Figure 4.33 Immunofluorescence staining using anti-GFP antibodies of methanol fixed SU557 (GFP-ZapA) outgrown spores..... 136

Figure 4.34 Model for the pathway of FtsZ polymerisation during the cell cycle, leading to establishment of the Z ring at the division site at midcell..... 139

Figure 4.35 Lipid helices in *B. subtilis*.. 145

Figure 5.1 Crystal structure of the MinC dimer from *Thermotoga maritima*..... 151

Figure 5.2 Localization of MinD in live *B. subtilis* cells. 152

Figure 5.3 Localization of DivIVA-GFP in germinating *B. subtilis* spores.154

Figure 5.4 Phase contrast image of wild type and SU573 (MinCD⁺⁺) cells.160

Figure 5.5 Western blot to test the polyclonal MinD antibody against wild type and MinCD deletion strains.164

Figure 5.6 Anti-FtsZ immunofluorescence staining of SU573 (MinCD⁺⁺) outgrown *B. subtilis* spores in the absence of inducer.166

Figure 5.7 Anti-FtsZ immunofluorescence staining of SU573 (MinCD⁺⁺) outgrown *B. subtilis* spores in the presence of IPTG.167

Figure 5.8 Immunofluorescence analysis of FtsZ localization in SU573 (MinCD⁺⁺)..170

Figure 5.9 Projected two-dimensional images of FtsZ structures in SU573 (MinCD⁺⁺) cells obtained by 3D deconvolution.171

Figure 5.10 Experimental strategy for the construction of a MinCD⁻ strain of *B. subtilis*. 174

Figure 5.11 Ethanol fixation of MinCD⁻ strains and SU8 wild type.....176

Figure 5.12 Immunofluorescence analysis of FtsZ localization in wild type and MinCD-null cells.177

Figure 5.13 Projected two-dimensional images of FtsZ structures in MinCD-null cells obtained by 3D deconvolution.179

Figure 5.14 Z ring positioning and immunofluorescence images of MinCD-null and wild type outgrown spores..182

Figure 5.15 Short interval time-lapse images of FtsZ-YFP localization in outgrowing spores of SU556 (MinCD⁻ FtsZ-YFP).186

Figure 5.16 Time-lapse images of FtsZ-YFP localization in outgrowing spores of SU556 (MinCD⁻ FtsZ-YFP) showing extended FtsZ helix.....188

Figure 5.17 Time-lapse images of FtsZ-YFP localization in outgrowing spores of SU556 (MinCD⁻ FtsZ-YFP) showing polar short FtsZ helix.190

Figure 5.18 Graph of FtsZ-YFP localization during the first cell cycle in outgrowing spores of SU556 (MinCD⁻ FtsZ-YFP).191

Figure 5.19 Time-lapse images of FtsZ-YFP localization in outgrowing spores of SU556 (MinCD⁻ FtsZ-YFP) showing polar and midcell Z ring formation.....192

Figure 5.20 Graph of FtsZ-YFP localization during the first cell cycle in an outgrown spore.....193

Figure 5.21 Extended time-lapse imaging of FtsZ-YFP localization in outgrowing spores of SU556 (MinCD⁻ FtsZ-YFP) showing minicell formation..195

Figure 5.22 Time-lapse images of FtsZ-YFP localization in vegetatively growing SU556 (MinCD⁻ FtsZ-YFP) showing minicell formation.197

Figure 5.23 Time-lapse images of FtsZ-YFP localization in outgrowing spores of SU556 (MinCD⁻ FtsZ-YFP) showing relocation of the Z ring.200

Figure 5.24 Z ring positioning of SU593 (MinCD⁺⁺ FtsZ-GFP) in the absence of IPTG. .203

Figure 5.25 Live fluorescence analysis of FtsZ-GFP localization in SU593 (MinCD⁺⁺ FtsZ-GFP) cells.....204

Figure 5.26 Western blot against the MinD protein in outgrowing wild type and SU593 (MinCD⁺⁺ FtsZ-GFP) spores.....206

Figure 5.27 Visualisation of FtsZ-GFP in SU593 (MinCD⁺⁺ FtsZ-GFP) outgrown spores not over-expressing MinCD.208

Figure 5.28 Visualisation of FtsZ-GFP in SU593 (MinCD⁺⁺ FtsZ-GFP) outgrown spores over-expressing MinCD..210

Figure 5.29 Z stacks of FtsZ-GFP in SU593 (MinCD ⁺⁺ FtsZ-GFP) outgrown <i>B. subtilis</i> spores.....	212
Figure 5.30 Time-lapse images of FtsZ-GFP localization in SU593 (MinCD ⁺⁺ FtsZ-GFP) outgrown spores without MinCD over-expression.	213
Figure 5.31 Time-lapse images of FtsZ-GFP localization in SU593 (MinCD ⁺⁺ FtsZ-GFP) in outgrown spores with MinCD over-expression.	214
Figure 5.32 FtsZ-GFP localization during two cell cycles in an SU593 (MinCD ⁺⁺ FtsZ-GFP) outgrown spore over-expressing MinCD.	216
Figure 5.33 Time-lapse images of FtsZ-GFP localization in SU593 (MinCD ⁺⁺ FtsZ-GFP) outgrown spores over-expressing MinCD, showing extended dynamics of the short midcell FtsZ helix.	218
Figure 5.34 Immunofluorescence analysis of MinC and MinD localization..	222
Figure 5.35 Model for the pathway of FtsZ polymerisation during the cell cycle in the absence of the Min system, leading to establishment of the Z ring at the polar division site.	225
Figure 5.36 Two alternative models proposing how the Z ring arises from a short helical FtsZ intermediate..	231
Figure 6.1 Comparison of the PSF of confocal and 4Pi microscopes.....	238
Figure 6.2 Shrinking the Focal Spot by STED microscopy.....	240
Figure 6.3 Depiction of the excitation and depletion lasers used to enhance resolution in STED microscopy..	241
Figure 6.4 Focal spots of confocal and STED and testing photo-bleaching.	242
Figure 6.5 Samples showing an increase of resolution when imaged with STED microscopy.	243
Figure 6.6 Preparative steps for 4Pi sample.....	246
Figure 6.7 1-photon 4Pi image of SU5 <i>B. subtilis</i> wild type cells.....	248
Figure 6.8 Rate of bleaching of the Alexa 488 dye in four separate regions in <i>B. subtilis</i> cells.	251
Figure 6.9 Characteristics of the ATTO 647N dye.	252
Figure 6.10 Absorbance graph of the antibody and dye conjugation reaction.....	253
Figure 6.11 Immunofluorescence analysis of FtsZ localization using the ATTO 647N dye..	255
Figure 6.12 Z ring positioning of SU5 using the ATTO 647N secondary antibody (Sigma)..	256
Figure 6.13 Immunofluorescence analysis of FtsZ localization using both confocal and STED imaging.....	258
Figure 6.14 Immunofluorescence analysis and characterisation of FtsZ localization using STED microscopy.	259
Figure 6.15 Analysis of STED images using fluorescence intensity graphs of wild type <i>B. subtilis</i> cells.....	261
Figure 6.16 An example of fast Fourier transform (FFT) analysis on a non-biological sample..	263
Figure 6.17 Immunofluorescence analysis of FtsZ localization using STED microscopy and fast Fourier transform (FFT) analysis showing 156-157 nm spacing.....	264
Figure 6.18 Immunofluorescence analysis of FtsZ localization using STED microscopy and fast Fourier transform (FFT) analysis..	265
Figure 6.19 Binding possibilities of primary and secondary antibodies to FtsZ..	266

Figure 6.20 Immunofluorescence analysis using STED microscopy of FtsZ localization with various secondary antibody concentrations.267

Figure 6.21 Calculation of the distances between the slide and the coverslip when using the STED setup..268

Figure 6.22 Calculation of actual FWHM of images resolved with STED microscopy. ...269

Figure 6.23 Model for FtsZ helix and ring formation in *B. subtilis*.273

Figure 6.24 Schematics of possible helical paths for FtsZ assembly within *B. subtilis*. ...276

Figure 6.25 Comparison of the focal spots of STED verses 4Pi, and the focal spot of a combined 4Pi/STED system.278

Figure 6.26 Image of membrane-labelled (with the styryl dye RH414) bacteria *Bacillus megaterium*.278

Table of Tables

Table 2.1 Commonly used aqueous buffers and solutions..... 37

Table 2.2 *B. subtilis* strains 38

Table 2.3 *B. subtilis* growth media..... 39

Table 2.4 Antibiotics used for selection in *B. subtilis*..... 39

Table 2.5 Primers used for PCR reactions. 44

Table 2.6 Antibodies used for primary and secondary detection for both IFM and western blot analysis..... 46

Table 3.1 Z ring positioning of SU8 and SU473 (HPUra^R) in the absence and presence of HPUra..... 74

Table 3.2 P values from the two sample t-test assuming unequal variances comparing the position of the Z ring in the strains SU8 and SU473 (HPUra^R) in the absence and presence of HPUra. 74

Table 4.1 Cell length measurements of ethanol fixed cells.. 118

Table 5.1 Cell length of SU5 and SU573 (MinCD⁺⁺) with and without IPTG induction of excess MinCD. 160

Table 5.2 Cell lengths of ethanol fixed SU573 (MinCD⁺⁺) cells grown in PAB with various concentrations of IPTG inducing MinCD over-expression. 161

Table 5.3 IFM against FtsZ on SU573 (MinCD⁺⁺) outgrown *B. subtilis* spores without IPTG (A), and with 1 mM IPTG (B)..... 168

Table 5.4 FtsZ localization in fixed IFM stained cells of SU560 (MinCD⁻) outgrown spores, and the wild type control, SU8..... 183

Table 5.5 Live FtsZ-YFP in SU556 (MinCD⁻ FtsZ-YFP) outgrown spores with 0.2% xylose. 184

Table 5.6 Analysis of time-lapse microscopy in SU556 (MinCD⁻ FtsZ-YFP).. 199

Table 5.7 Cell length of live SU593 (MinCD⁺⁺ FtsZ-GFP) with 1 mM IPTG inducing over-expression of MinCD, analysing frequency of Z ring formation by FtsZ-GFP visualisation. 205

Table 5.8 Live FtsZ-GFP in SU593 (MinCD⁺⁺ FtsZ-GFP) outgrown *B. subtilis* spores without IPTG (A), and with 1 mM IPTG (B).. 211

Table 5.9 Analysis of time-lapse microscopy in SU593 (MinCD⁺⁺ FtsZ-GFP) without (wild type) and with 1 mM IPTG (over-expressed). 220

Table 6.1 Analysis of STED images using fluorescence intensity graphs of wild type *B. subtilis* cells..... 262

Publications

Journal articles

Phoebe C. Peters, Margaret D. Migocki, Carola Thoni and Elizabeth J. Harry. (2007). A new assembly pathway for the cytokinetic Z ring from a dynamic helical structure in vegetatively growing cells of *Bacillus subtilis*. *Molecular Microbiology* **64(2)**, 487-499

Phoebe C. Peters, Carola Thoni and Elizabeth J. Harry. (2006). Unexpected photo-bleaching of Alexa488 in a fixed bacterial sample occurring during 2-photon excitation. *Biotechnic and Histochemistry* **81**, 105-106

Conference proceedings

Peters, P.C. and Harry, E.J. (June 2008). Examining the relationship between the Min system and the FtsZ helix. **POSTER**, Gordon Cell Surfaces Conference, New London, New Hampshire, USA.

Peters, P.C. and Harry, E.J. (November 2007) Bacterial Cell Division: Identifying the Midcell Site. **SEMINAR-026**, 24th Annual Scientific Research Meeting, Sydney, Australia

Peters, P.C., Thoni C. and Harry, E.J. (July 2007) A Cell-Cycle Regulated Helical Structure of FtsZ in *B. subtilis*. **PLENARY SEMINAR-04-4**, ASM2007 Annual ASM Scientific Meeting, Adelaide, Australia.

Peters, P.C. Migocki, M.D., and Harry, E.J. (August 2006). A cell-cycle regulated helical structure of FtsZ in *B. subtilis*. **POSTER**, EMBO Cell Cycle and Cytoskeletal Elements in Bacteria, Copenhagen, Denmark.

Peters, P.C., Thoni, C. and Harry, E.J. (February 2006). A time-lapse microscopy revelation: The dynamic helical nature of the bacterial division protein FtsZ. **POSTER-4**, Biophotonics in Australia Showcase and Strategic Planning, Sydney, Australia

Peters, P.C., Migocki, M.D., and Harry, E.J. (November 2005). A new twist to bacterial cell division: spiral forms of FtsZ. **POSTER**, UTS Science Faculty Forum, Sydney, Australia (Recipient of poster prize).

Peters, P.C., Migocki, M.D., and Harry, E.J. (September 2005). A new twist to bacterial cell division: spiral forms of FtsZ. **POSTER-MON-029**, ComBio2005, 49th Annual ASBMB Conference, Adelaide, Australia

Grants

Liz Harry, Carola Thoni and **Phoebe Peters** (late 2007). Bacterial Cell Biology: Investigating an optical revolution. From ARC network FABLS (Fluorescence Applications in Biotechnology and Life Sciences)

Abbreviations

A#	absorbance (# refers to the wavelength in nm)
A	alanine
aa	amino acid
Ab	antibody
AGRF	Australian Research Genome Facility
AP	alkaline phosphatase
ARC	Australian Research Council
ATM	atomic force microscopy
B.	<i>Bacillus</i>
β	beta
bp	base pair(s)
BP	band pass
BSA	bovine serum albumin
cm	centimeters
Cm ^R	chloramphenicol resistance
CCD	charged coupled device
DAPI	4'6-diamidino-2-phenylindole
dATP	deoxyadenosine 5'-triphosphate
dCTP	deoxycytidine 5'-triphosphate
dGTP	deoxyguanosine 5'-triphosphate
DIC	differential interference contrast
DOL	degree of labelling
DNA	deoxyribonucleic acid
DNA pol	DNA polymerase III holoenzyme
dpm	decays per minute
dsDNA	double stranded deoxyribonucleic acid
DTT	dithiothreitol
dTTP	deoxythymidine 5'-triphosphate
DVD	digital versatile disc
E.	<i>Escherichia</i>

ECT	electron cryotomography
<i>et al.</i>	and others
FABLS	Fluorescence Applications in Biotechnology and Life Sciences
FAD	flavin adenine dinucleotide
FFT	Fourier transform analysis
FITC	fluorescein isothiocyanate
FRAP	fluorescence recovery after photobleaching
FRET	fluorescence energy resonance transfer
<i>fts</i>	filamentation temperature sensitive
FWHM	full width half maximum
<i>g</i>	centrifugal force
<i>g</i>	gram(s)
GFP	green fluorescent protein
GMD	germination medium defined
hr	hour(s)
HPUra	6-(<i>p</i> -hydroxyphenylazo)-uracil
HPUra ^R	HPUra resistant
IFM	immunofluorescence microscopy
IgG	Immunoglobulin G
IPTG	isopropyl-1-thio- β -D-galactopyranoside
kD	kilo Dalton(s)
L	litre(s)
LP	long pass
m	milli- (10^{-3})
M	moles per litre
min	minute(s)
MQW	Milli-Q purified water
MSA	mineral salts A
MTS	membrane targeting sequence
n	nano- (10^{-9})
NA	numerical aperture
N/A	not applicable

NHS	N-hydroxysuccinimide
NO	nucleoid occlusion
NS	nucleation site
OD	optical density
<i>P</i>	probability
<i>P_{spac}</i>	IPTG-inducible promoter
<i>P_{spac-hy}</i>	IPTG-hyper-inducible promoter
<i>P_{xyl}</i>	xylose-inducible promoter
PAGE	polyacrylamide gel electrophoresis
PBS	phosphate buffered saline
PCR	polymerase chain reaction
pers. comm.	personal communication
pH	power of Hydrogen
PSF	point spread function
RNA	ribonucleic acid
RNase	ribonuclease A
ROR	round of replication
ROW	reverse osmosis purified water
rpm	revolutions per minute
<i>S.</i>	<i>Streptomyces</i>
S	serine
sec	second(s)
SDS	sodium dodecyl sulfate
SEM	standard error of the mean
SMC	structural maintenance of chromosome
SMM	spizizen minimal medium
spp.	species
spec	spectinomycin
STED	Stimulated emission depletion
T	thymine
TBAB	tryptose blood agar base
TBP	tributyl phosphate

TDE	2,2'-thiodiethanol
TEMED	N,N,N',N'-tetramethyl-ethylenediamine
tet	tetracycline
TFA	trifluoroacetic acid
thy ⁻	thymine auxotroph
Tris	tris(hydroxymethyl)methylamine
Trp	L-Tryptophan
ts	temperature sensitive
U	units (enzyme activity)
UV	ultraviolet
V	volt(s)
v/v	volume per volume
W	watt
w/v	weight per volume
YFP	yellow fluorescent protein
2D	2-dimensional
3D	3-dimensional
4D	4-dimensional
μ	micro- (10 ⁻⁶)
μCi	micro curie

Abstract

As with all organisms, bacterial cells divide with amazing precision. The first stage of this process is marked by the polymerisation of the essential tubulin-like FtsZ protein at midcell into a ring, the Z ring. Understanding its formation and regulation provides an insight into how the crucial event of cell division is controlled. However, despite intense investigation, these molecular mechanisms are not fully understood. One factor believed to play a role in midcell Z ring placement is the coordination between DNA replication and cell division. Previously it has been shown that when initiation of DNA replication is allowed, but DNA synthesis is inhibited by two different methods (thymine starvation or addition of HPUra), Z rings are able to form at midcell in one case, and not in the other. Both conditions block DNA synthesis at the same stage, the beginning of DNA chain elongation. In an attempt to understand these incongruous results, the possibility of the drug HPUra playing a non-replicative role, leading to displacement of the Z ring, was examined. It was found that Z ring positioning in an HPUra-resistant strain was not significantly different to that of wild type. Z rings formed at midcell in both conditions. Thus in the wild type strain, the effect of HPUra on Z ring positioning is dependant on its ability to inhibit replication. Hence the block to the elongation stage of DNA replication mediated by the addition of HPUra is capable of misplacing the Z ring, strong evidence for a link between these essential processes of DNA replication and cell division.

Ten years ago it was proposed that the Z ring forms by bidirectional growth from a midcell nucleation site. Work presented in this thesis now suggests this may not be the case. Using a modified immunofluorescence protocol it was discovered that, in addition to forming a Z ring, FtsZ forms a helical structure along the length of the cell in vegetatively growing wild type *Bacillus subtilis* cells. Time-lapse experiments in live cells using an inducible FtsZ-YFP fusion, showed that the helical FtsZ structure is highly dynamic and undergoes cell cycle-regulated changes in localization. The monitoring of a complete cell cycle revealed the early appearance of a pole-to-pole FtsZ helix, a subsequent short helix spatially restricted to midcell, and finally this redistributed to produce a sharp midcell Z ring. These observations led to the proposal of a novel assembly mechanism for Z ring formation

involving a cell-cycle mediated multi-step remodelling of FtsZ polymers. This was the first report of an FtsZ helix in *B. subtilis* during vegetative growth.

The new model for Z ring formation predicts that in order for the cell to assemble a Z ring, FtsZ must go through long helix-to-short helix-to-Z ring polymerisation changes. How is the Min system, a known negative regulator of FtsZ responsible for inhibiting aberrant Z ring assembly at the cell poles, involved in regulating these FtsZ polymerisation transitions? To address this, FtsZ polymer remodelling was examined whilst modifying the effect of the Min system. Time-lapse studies of a strain carrying a deletion of the *minCD* genes showed FtsZ polymerising at the poles in the same fashion as wild type; that is going through a short helical intermediate prior to Z ring formation. This indicated that the helical form of FtsZ is in fact a true intermediate, required for Z rings to form even at non-midcell locations. A *minCD* over-expression strain showed a marked decrease in Z ring formation and time-lapse imaging was conducted to assess at which transitional stage FtsZ assembly was affected. Interestingly, it was found that both the long and short helical polymerisations of FtsZ can actually form as wild type in the over-expression experiments. The excess of MinCD in the cell appeared to be able to severely impair division by hampering and prolonging the transition of the short midcell helix to a ring. It is proposed that this is mediated by the inhibition of lateral interactions of FtsZ protofilaments. Indeed a model is put forth emphasizing the importance of lateral interactions in the helix-to-ring remodelling, and thus in stable Z ring formation.

To examine the *in vivo* FtsZ helix with higher resolution, the advanced microscopic techniques of 4Pi and STED imaging were employed. Using alternative methods has the advantages of confirming the helical structure and extracts further information, for example is the helix continuous? STED microscopy breaks the diffraction barrier and lateral resolution is increased to ~100 nm, ~2.5 times that of normal confocal microscopy. Using STED, FtsZ localization showed a distinct periodicity, consistent with a helical conformation. Additionally FtsZ staining was revealed to be extremely punctate and discontinuous, suggesting that the helical structure of FtsZ may depend on a cellular track. Visualising cells and their sub-cellular structure in ever increasing detail ensures novel insights into the regulation of Z ring assembly in bacteria.